Published in final edited form as:
Nat Immunol. 2010 June ; 11(6): 503–511. doi:10.1038/ni.1868.

Regulation of thymocyte positive selection and motility by GIT2

Hyewon Phee[1], **Ivan Dzhagalov**[3], **Marianne Mollenauer**[1,2], **Yana Wang**[4], **Darrell J. Irvine**[5,6], **Ellen Robey**[3], and **Arthur Weiss**[1,2]

[1]Department of Medicine, Division of Rheumatology, University of California San Francisco, San Francisco, CA 94143

[2]Howard Hughes Medical Institute, Rosalind Russell Medical Research Center for Arthritis, University of California San Francisco, San Francisco, CA 94143

[3]Department of Molecular and Cell Biology, Division of Immunology and Pathogenesis, University of California Berkeley, Berkeley, CA 94720

[4]Department of Chemical Engineering, Massachusetts Institute of Technology, Cambridge, MA 02139

[5]Departments of Biological Engineering and Materials Science and Engineering, Massachusetts Institute of Technology, Cambridge, MA 02139

[6]Howard Hughes Medical Institute, Chevy Chase, MD 20815

Abstract

Thymocytes are highly motile cells that migrate under the influence of chemokines in distinct thymic compartments as they mature. The motility of thymocytes is tightly regulated; however, the molecular mechanisms that control thymocyte motility are not well understood. Herein, we report that G protein-coupled receptor kinase-interactor 2 (GIT2) is required for efficient positive selection. Interestingly, GIT2$^{-/-}$ double positive (DP) thymocytes display increased Rac activation, actin polymerization and migration towards SDF-1 and CCL25 *in vitro*. Using two-photon laser scanning microscopy, we found that scanning activity of GIT2$^{-/-}$ thymocytes is severely compromised in the thymic cortex, suggesting GIT2 plays a key role in regulating chemokine-mediated motility of DP thymocytes.

Introduction

Migration signals serve a fundamental function in the development of thymocytes. As thymocytes travel to distinct sites in the thymus, they undergo selection, differentiation and proliferation until they are mature and are finally exported into the blood[1]. Transition between sites in the thymus and stages of development depends on interactions with resident cells found in distinct compartments[1]. For example, DP thymocytes interact with thymic epithelial cells in the cortex (cTECs) and undergo positive selection using their newly assembled TCRs to recognize self peptide-major histocompatibility (pMHC) proteins expressed by the cTECs. The majority of DP thymocytes die because they fail to receive appropriate signals from TCR-pMHC interactions. A small number of DP thymocytes are

Corresponding author: Arthur Weiss, UCSF, HHMI, Box 0795, S-1024, 513 Parnassus, San Francisco, CA 94143-0795, aweiss@medicine.ucsf.edu, phone: (415) 476-1291, FAX: (415) 502-5081.

Author Contributions

H.P. designed the study, did experiments, analyzed data and wrote the manuscript; M.M. did experiments; I.D did two photon experiments and analyzed data; Y.W. and D.I. supplied alginate beads; E.R. supervised the two-photon experiments and discussed data; and, A.W. designed the study, supervised the research and revised the manuscript.

successfully positively selected and differentiate into CD4 or CD8 single positive (SP) thymocytes.

Motility and interaction of DP thymocytes with cTECs are important factors in positive selection. The motile nature of thymocytes facilitates their search for potentially rare TCR-reactive pMHC molecules on cTECs. Multiple interactions with distinct cTECs may occur, but at the same time, DP thymocytes must integrate the individual signaling events that occur as a result of such interactions with cTECs in order to initiate fate decisions. Thus, maintaining a fine balance between motility and duration of interactions with cTECs may be critical for successful positive selection. Recent advances in two-photon laser scanning microscopic imaging have shed light on the motility and interaction behavior of DP thymocytes during positive selection in the cortex[1–5]. One study revealed that the vast majority of DP thymocytes move randomly at relatively low motility rates of 3–8 μm/min[3]. Frequent pausing and turning back towards the cell's origin was observed in the DP thymocyte population, suggesting they travel in a random fashion and extensively interact with their environment. In another study[4], TCR transgenic DP thymocytes on a positively selecting background displayed increased duration of interactions with cTECs compared with DP thymocytes on a non-selecting background. Positive selection was correlated with greater calcium oscillations that negatively regulated thymocyte motility[4]. These observations predict that, if thymocyte-stromal cell interactions are altered, for example, by changes in chemokine-mediated motility signals, the efficiency of positive selection might be compromised. The functional consequences of disrupting proper motility and the molecules that regulate DP thymocyte motility are not well understood.

Chemokines such as CCL25 (also known as TECK; T cell Expressed ChemoKine) or SDF-1 (stromal cell derived factor-1; CXCL12) are expressed throughout the thymic cortex[6–8], and their receptors, CCR9 and CXCR4, are expressed highly in DP thymocytes[9]. However, the migratory response of thymocytes is not simply dictated by the level of chemokine receptor expression. For instance, pre-selection DP thymocytes do not migrate efficiently to CCL25 despite the fact that expression of CCR9 is similar on non-selected $CD69^{low}$ versus positively selected $CD69^{high}$ DP cells[10,11]. Positively selecting signals from the TCR-pMHC interaction may therefore render thymocytes more responsive to CCL25[10].

The GIT family of proteins, comprised of GIT1 and GIT2, are multifunctional proteins characterized by the N-terminal GTPase activating protein (GAP) domain for ADP-ribosylation factor (Arf) family of small GTP-binding proteins[12–16]. In peripheral T cells and thymocytes, GIT2 is the predominantly expressed isoform. GIT1 and GIT2 display Arf GAP activity towards Arf1 and Arf6[17, 18], which influence membrane traffic and actin remodeling[14]. Interestingly, Arf6 has been specifically implicated in the formation of actin-rich protrusions and membrane ruffles by activating Rac[19, 20, 21]. GIT proteins interact with multiple molecules such as GPCR kinases (GRKs)[22], PIX (PAK interacting exchange factor)[23] or paxillin[24] and serve a pivotal role in focal adhesion disassembly[15], cell polarity and directional motility in migrating adherent cells[25], neuronal cells[26], and neutrophils[13, 27]. Part of GIT's function may stem from its ability to repress Rac activation. For instance, GIT2 represses Rac-dependent lamellipodia extension and cell spreading in HeLa cells[25]. In migrating adherent cells, integrin α4-mediated GIT1 recruitment to the lateral sides and trailing edge restricts Rac activation allowing Rac activation at the leading edge[28].

Although GIT2 is crucial in the regulation of cell migration, adhesion and polarity in non-hematopoietic cells, our understanding of the role of GIT2 in T cells is very limited. Previously, our laboratory showed that GIT interacts with PIX and PAK constitutively in a tri-molecular complex in T cells[29]. We found that the GIT-PIX-PAK complex is recruited to the T cell immunological synapse and this recruitment is mediated by PIX[30]. Although these

findings revealed that PIX plays a role in recruiting PAK to the immunological synapse, it is not clear what specific role GIT2 plays in T cell function or development. Because rapid cytoskeletal rearrangement is fundamental for T cell motility, adhesion, APC recognition, and changes in morphology, it is possible that the GIT2 plays a role in T cell cytoskeletal reorganization.

Here, we report that generation of mature CD4 SP thymocytes in TCR transgenic GIT2$^{-/-}$ mice is severely impaired due to inefficient positive selection. However, the TCR signaling ability of GIT2$^{-/-}$ thymocytes that is critical for positive selection is unimpaired. Likewise, cell death and apoptosis are not altered in GIT2$^{-/-}$ thymocytes. Instead, we found that migration in response to SDF-1 and CCL25 *in vitro* by GIT2$^{-/-}$ DP thymocytes is increased. Furthermore, in response to SDF-1 GIT2$^{-/-}$ thymocytes exhibit increased motility in a collagen matrix, exaggerated Rac activation and actin polymerization. Increased numbers of GIT2$^{-/-}$ DP thymocytes migrate to SDF-1 in the presence of a TCR-mediated stop signal. To determine how the inappropriate chemokine response of GIT2$^{-/-}$ thymocytes affects thymocyte motility *in vivo*, we utilized two photon laser scanning microscopy (TPLSM) to monitor the migratory behavior of WT and GIT2$^{-/-}$ thymocytes in intact thymic lobes. Paradoxically, we observed decreased motility of GIT2$^{-/-}$ thymocytes, accompanied by an accumulation of GIT2$^{-/-}$ thymocytes in certain areas of the cortex including adjacent to SDF-1 positive small blood vessels. We propose that the *in vivo* migratory defect of the GIT2$^{-/-}$ thymocytes is a steady state consequence of trapped thymocytes resulting from an exaggerated response to local chemokine gradients in the cortex, thus compromising their ability to receive proper TCR signals required for efficient positive selection.

Results

Generation of GIT2-deficient mice

To determine the roles of GIT2 *in vivo*, we generated GIT2$^{-/-}$ mice using an available gene-trapped embryonic stem (ES) cell line. The insertion site of the retroviral vector was confirmed by genomic sequencing of ES cells (Supplementary Fig. 1a). GIT2$^{-/-}$ mice were born healthy at normal Mendelian ratios. We examined GIT2 mRNA expression from the spleen and thymus of WT, heterozygote and homozygote mice for the trapped GIT2 gene. Targeted mice have more than a 90% reduction in GIT2 mRNA compared to WT (Supplementary Fig. 1b). The remaining 10% expression of mRNA is likely due to alternative splicing. Likewise, protein expression was more than 90% reduced in the thymus of homozygous GIT2 gene-trapped mice (Supplementary Fig. 1c). GIT proteins exist in two forms, GIT1 and GIT2. GIT1 is highly expressed in the brain and expressed in much lower amounts in the thymus and spleen compared to GIT2, establishing GIT2 as the major isoform expressed in T cells[31] (Supplementary Fig. 1c, 1d). Thus, we focused on determining the role of GIT2 in T cells.

The GIT2$^{-/-}$ line was backcrossed 9 generations to C57BL/6 and BALB/c backgrounds. GIT2$^{-/-}$ mice on either background do not manifest any substantial change in T and B cell populations in the thymus, spleen and lymph nodes except that the number and percentage of marginal zone B cells was increased (Supplementary Fig. 2a, 2b).

CD4 SP cell number is reduced in TCR transgenic GIT2$^{-/-}$ mice

Developmental defects associated with thymocyte selection can be masked by compensatory changes in the TCR repertoire. Thus, to better define the alterations in thymocyte development, we introduced single αβTCR transgenes into WT and GIT2$^{-/-}$ mice to limit compensation. Two independent MHC class II-restricted TCR (ovalbumin peptide-specific DO11.10 and OTII, respectively) transgenic models were used. In contrast to WT DO11.10

or OTII transgenic mice, the numbers and percentages of CD4 SP cells were greatly reduced in both DO11.10 (Fig. 1a, 1b) and OTII transgenic GIT2$^{-/-}$ thymi (Supplementary Fig. 3a, 3b). The population with the greatest reduction in DO11.10+ GIT2$^{-/-}$ thymocytes was the mature TCR transgene hi (KJ1-26 hi) population, which is comprised mainly of CD4 SP thymocytes (Fig. 1c; Supplementary Fig. 3c for OTII). CD4 SP development in the thymus is the result of positive selection which occurs at the DP stage. Small numbers of DP thymocytes that have undergone positive selection up-regulate CD69 and CD3/TCR transgene. The KJ-126^{hi}/CD69^{hi} population of DP thymocytes was consistently decreased in DO11.10+GIT2$^{-/-}$ mice (Fig. 1d). Consistent with this decrease of CD4 SP thymocytes, the percentages and numbers of transgene positive peripheral CD4 T cells in the spleen, lymph node and blood were greatly reduced in TCR transgenic GIT2$^{-/-}$ mice (Fig. 1e, 1f, Supplementary Fig. 3d, data not shown).

Impaired positive selection results in reduced CD4 SP cell numbers in TCR transgenic GIT2$^{-/-}$ mice

To assess the efficiency of generating CD4 SP thymocytes from DP thymocytes, mice were exposed to continuous BrdU incorporation *in vivo* (Fig. 2a). The percentages of BrdU positive cells in DP population were similar in TCR transgenic WT and GIT2$^{-/-}$ thymocytes. However, the percentage of BrdU positive cells in the CD4 SP population was markedly reduced in TCR transgenic GIT2$^{-/-}$ mice, suggesting that the generation of CD4 SP thymocytes is impaired.

It is possible that the reduction of CD4 SP thymocytes is due to an increase in cell death or apoptosis in TCR transgenic GIT2$^{-/-}$ mice. To examine this possibility, we stained thymocytes with Annexin V and 7AAD after 4 and 24 hours of incubation in 10% FBS media (Fig. 2b) or with CD3 and CD28 (data not shown). We also did not detect any substantial increase in cell death or apoptosis between TCR transgenic WT and GIT2$^{-/-}$ DP or SP thymocytes. Moreover, we measured the level of active caspase 3 by intracellular staining in TCR transgenic WT or GIT2$^{-/-}$ mice and the percentages of active caspase 3 positive cells were similar in all subsets from TCR transgenic WT and GIT2$^{-/-}$ thymocytes (Fig. 2c).

To examine the possibility that the absence of GIT2 affects negative selection, we introduced the H-Y TCR transgene into GIT2$^{-/-}$ mice. H-Y TCR transgenic mice express a TCR specific for the male H-Y antigen presented in the context of the H-2D^{b} MHCI molecule. Thymocytes bearing the transgenic TCR are positively selected in females but deleted by negative selection in male mice[32, 33]. We did not detect any difference in negative selection in H-Y male GIT2$^{-/-}$ thymus as compared to WT (Supplementary Fig. 3e, 3f). In contrast, the generation of CD8 SP thymocytes in female H-Y TCR transgenic GIT2$^{-/-}$ mice was impaired, suggesting that positive selection on MHCI is also disrupted in the absence of GIT2 (data not shown). To further examine whether increased negative selection occurs in the CD4 or CD8 SP stage in the thymus or in the periphery, Vβ expression was measured on WT or GIT2$^{-/-}$ mice on the BALB/c background. Deletion of certain Vβ TCR expressing cells occurs in the BALB/c background due to endogenous superantigen expression. However, we found no evidence for altered deletion of cell expressing Vβ3, 5 or 11 TCRs in GIT2$^{-/-}$ mice in the thymus, spleen and lymph nodes (Fig. 2d and data not shown). We conclude that increased cell death or increased negative selection does not account for the reduced number of transgene-TCR expressing CD4 SP thymocyte GIT2$^{-/-}$ thymocytes. Thus, GIT2 function is required for efficient positive selection under conditions when TCR affinity is fixed.

Defective generation of CD4 SP thymocytes in TCR transgenic GIT2$^{-/-}$ mice is hematopoietic cell intrinsic

To determine whether the defect in generating CD4 SP cells in TCR transgenic GIT2$^{-/-}$ thymus is hematopoietic cell intrinsic, we generated chimeras that were reconstituted with either DO11.10+WT or DO11.10+GIT2$^{-/-}$ bone marrow (Fig. 3a). All thymocyte subsets from the WT chimera developed properly. However, the generation of CD4 SP thymocytes from DO11.10+GIT2$^{-/-}$ bone marrow was substantially reduced. We examined thymic architecture of DO11.10+WT or DO11.10+GIT2$^{-/-}$ chimeras. Because CD4+ SP thymocytes were significantly reduced in DO11.10+ GIT2$^{-/-}$ chimera, the thymic medulla was substantially smaller compared to thymus from DO11.10+WT chimera (Fig. 3c). In addition, we determined whether non-hematopoietic cells from GIT2$^{-/-}$ thymus contributed to impaired positive selection. We generated chimeras using WT or GIT2$^{-/-}$ mice as hosts and DO11.10+WT bone marrow as the donor. However, we did not detect any difference between WT and GIT2$^{-/-}$ hosts reconstituted with DO11.10+WT donor (Fig. 3b), suggesting that non-hematopoietic cells from GIT2$^{-/-}$ mice are able to provide a thymic environment that fosters proper thymocyte development. Next, we performed competitive repopulation experiments of the thymus in lethally irradiated hosts. Using OTII+ WT (CD45.1/CD45.2) and OTII+ GIT2$^{-/-}$ (CD45.2/CD45.2) donor BM cells, 1:1 mixed chimera were generated. After 2 months, reconstitution of the two donor populations was measured at the DN, DP and CD4 SP thymocyte stages. Injection of equal amounts of bone marrow stem cells resulted in roughly equal representation at the DN stage (55% OTII+WT and 45% OTII+GIT2$^{-/-}$) (Fig. 3d), suggesting WT and GIT2$^{-/-}$ thymic progenitors enter the thymus and generate DN thymocytes similarly. At the DP stage in OTII+WT and OTII +GIT2$^{-/-}$ mixed chimera, the representation of OTII+WT and OTII+ GIT2$^{-/-}$ thymocytes was slightly shifted in favor of OTII+WT population (60% OTII+WT and 40% OTII +GIT2$^{-/-}$). However, when the OTII+GIT2$^{-/-}$ population at the DN stage is compared to the OTII+GIT2$^{-/-}$ population at the DP stage, reconstitution from OTII+GIT2$^{-/-}$ donor cells was not significantly changed between the two stages (P=0.56). In marked contrast, at the CD4 SP stage and subsequent mature peripheral populations in the spleen, lymph nodes and blood, OTII+GIT2$^{-/-}$ cells were substantially underrepresented compared to OTII+WT cells, suggesting that OTII+GIT2$^{-/-}$ thymocytes have an intrinsic developmental disadvantage at the transition from the DP to the CD4 SP stage. Together, these data reveal that defective generation of CD4 SP thymocytes and CD4 T cells in the periphery in TCR transgenic GIT2$^{-/-}$ mice is hematopoietic cell intrinsic.

TCR-induced ERK activation and changes in intracellular calcium concentration are unaltered in GIT2$^{-/-}$ thymocytes

Defects in positive selection are often due to impaired TCR-induced signaling events at the DP stage. To determine whether GIT2 deficiency impairs TCR-mediated signal transduction, we examined ERK activation following TCR stimulation. Since Erk plays a key role in positive selection, we assessed ERK activation by phospho-flow analysis by gating on DP or CD4 SP populations. We did not detect any substantial defects in ERK activation in DP (Supplementary Fig. 4a) or CD4 SP thymocytes (data not shown). Global tyrosine phosphorylation and p38 MAPK activation following TCR stimulation were similar in WT and GIT2$^{-/-}$ thymocytes (data not shown). We also failed to detect alterations in intracellular calcium increase following TCR stimulation in either the GIT2$^{-/-}$ DP or CD4 SP subsets (Supplementary Fig. 4b). CD5 expression at the DP stage is proportional to the TCR signaling strength[34] and was only slightly decreased in DO11.10+GIT2$^{-/-}$ DP thymocytes (Supplementary Fig. 4c, 4d). GIT2 interacts with PIX and PAK (via PIX). To determine whether the association of PIX and PAK is affected by GIT2 deficiency, we immunoprecipitated PAK2 from resting or TCR- stimulated WT and GIT2$^{-/-}$ thymocytes and immunoblotted with anti-α/β PIX and anti-p95 PKL antibody (which recognizes both

GIT1 and GIT2) (Supplementary Fig. 5a). We found that PAK2 interacted with α/β PIX similarly in the presence or absence of GIT2. We also found that *in vitro* kinase activity of PAK2 was not changed in the absence of GIT2 following TCR stimulation (Supplementary Fig. 5b). Rac activation was also similar in WT and GIT2$^{-/-}$ thymocytes after TCR stimulation (Supplementary Fig. 5c). Collectively, these experiments suggest that TCR-induced signaling events leading to ERK, p38 MAPK, PAK2 and Rac activation and Ca^{2+} mobilization are intact in GIT2$^{-/-}$ thymocytes.

GIT2 negatively regulates T cell motility

Since GIT2 has been implicated in cellular processes that govern cell migration in non-hematopoietic cells, we determined whether the GIT2 deficiency affects thymocyte motility. First, we examined thymocyte migratory responses to the chemokines SDF-1 and CCL25 (Fig. 4a). We found that migration of GIT2$^{-/-}$ thymocytes is greatly increased in response to these chemokines, with the DP subset thymocytes from GIT2$^{-/-}$ mice showing the most substantial increase. We also consistently found that in the absence of any stimulus, basal migration was modestly increased in CD4 and CD8 SP subsets of GIT2$^{-/-}$ thymocytes. CD4 and CD8 SP thymocytes express high levels of CCR7, the receptor for CCL19 (EBI1-ligand chemokine; ELC) and CCL21 (Secondary Lymphoid-Tissue Chemokine; SLC), and migrate efficiently to these chemokines. Migration responses towards CCL19 and CCL21 were comparable in WT and GIT2$^{-/-}$ thymocytes, suggesting the increases in migration of GIT2$^{-/-}$ thymocytes are specific to CCL25 and SDF-1 (Supplementary Fig. 6a). Expression levels of chemokine receptors for SDF-1, CCL25, or ELC/SLC-CXCR4, CCR9, and CCR7 respectively-were similar in WT and GIT2$^{-/-}$ DP and CD4 SP thymocytes (Supplementary Fig. 6b).

Although all DP thymocytes express a similar level of the receptor for CCL25, CD69^{hi} DP thymocytes exhibit enhanced migration to CCL25[10, 11, 35]. Because GIT2$^{-/-}$ DP thymocytes display increased migration towards CCL25 and SDF-1, we determined which population of DP thymocytes is responsible for the increased response. The CD69^{hi}/TCRβ^{hi} subset of DP thymocytes represents a small population that has been positively selected ("post-selection DP thymocytes"), while the majority of DP thymocytes are CD69^{low}/TCRβ^{low} and have not undergone positive selection process ("pre-selection DP thymocytes"). Almost 50% of the WT DP cells that migrated in response to CCL25 are post-selection DP thymocytes (Fig. 4b). This indicates that over 40% of input WT post-selection DP thymocytes migrated to CCL25 (Fig. 4c). WT preselection DP thymocytes do not migrate as efficiently, resulting in only 10% of the input cells migrating in response to CCL25 (Fig. 4c). In contrast, the majority of migrated GIT2$^{-/-}$ DP thymocytes are pre-selection DP thymocytes(Fig. 4b). Twenty six percent of input GIT2$^{-/-}$ pre-selection DP thymocytes migrated in response to CCL25, resulting in a 2.6-fold increase compared to the same population of WT DP thymocytes (Fig. 4c). GIT2$^{-/-}$ post-selection DP thymocytes also showed increased migration to CCL25, although it was less prominent compared to the pre-selection population. Similar differences in migratory behavior were observed in GIT2$^{-/-}$ pre-selection DP thymocytes in response to SDF-1, resulting in a 3- fold increase in migration compared to WT (Fig. 4c). These results demonstrate that GIT2 suppresses the migration of DP thymocytes to CCL25 or SDF-1, especially at the stage prior to positive selection.

GIT2 deficiency increases directional and random motility of DP thymocytes

Chemokines enhance directional (chemotaxis) as well as random migration (chemokinesis). Because we consistently observed that the migration of GIT2$^{-/-}$ thymocytes in the absence of any added chemokine was modestly increased, it is possible that increased migration of GIT2$^{-/-}$ thymocytes in response to SDF-1 or CCL25 simply reflects increased chemokinesis. To distinguish chemokinesis from chemotaxis, we examined thymocyte

migration from the upper transwell under conditions in which SDF-1 is added to: 1) the bottom well only; 2) the upper well only; or, 3) both the top and bottom wells. If increased migration of GIT2$^{-/-}$ thymocytes to SDF-1 is simply due to increased chemokinesis, migration under conditions when SDF-1 is added to the upper well or both wells should be similar to when SDF-1 is added to the bottom well. We found that when SDF-1 was added to the top well or to both wells, GIT2$^{-/-}$ thymocytes exhibited increased migration compared WT, suggesting that chemokinesis of GIT2$^{-/-}$ thymocytes is indeed increased (Figure 5a). However, GIT2$^{-/-}$ thymocytes migrated best when SDF-1 was added only to the bottom well to generate a chemokine gradient, suggesting that directional migration is indeed increased in GIT2$^{-/-}$ thymocytes.

To further examine whether GIT2 deficiency increases directional motility, we measured directional migration of WT and GIT2$^{-/-}$ thymocytes on a two-dimensional ICAM-1 coated surface using SDF-1 releasing alginate beads and time-lapse fluorescence microscopy. Alginate beads can be used to adsorb SDF-1 and then release SDF-1 in a controlled manner[36]. We labeled WT and GIT2$^{-/-}$ thymocytes with CFSE and CMTMR, respectively, and let them migrate on the ICAM-1 coated surface in the presence of control beads or beads that were loaded with SDF-1. We found that both WT and GIT2$^{-/-}$ thymocytes sensed SDF-1 releasing beads and migrated towards them, suggesting directional sensing to SDF-1 is intact in the absence of GIT2 (Supplementary Fig. 7. and Supplemental Movie 1). We also measured directional migration on a two-dimensional ICAM-1 coated surface overlaid with collagen matrix to prevent convection. We analyzed the trajectory of WT or GIT2$^{-/-}$ thymocytes in the presence of non-loaded or SDF-1-loaded beads and measured their average speed (Figure 5b). When non-loaded beads were added, the average migration speed for WT and GIT2$^{-/-}$ thymocytes was 2.4 and 2.5 μm/min. In the presence of SDF-1 releasing beads, the average migration speed was increased for both WT and GIT2$^{-/-}$ thymocytes, but the average migration speed of GIT2$^{-/-}$ thymocytes was significantly higher than that of WT thymocytes (3.9 μm/min (WT) vs. 4.8 μm/min (GIT2$^{-/-}$); *, P=0.03). Since the velocity of thymocytes was heterogeneous, we binned the migration speed to visualize the range of increased migration of GIT2$^{-/-}$ thymocytes (Figure 5c). Interestingly, there were more GIT2$^{-/-}$ thymocytes migrating at the velocity range between 4–6 μm/min, which is consistent with migration rates of DP thymocytes (3–8 μm/min) as previously reported[3]. To quantify directional motility, we measured the directionality index (displacement divided by path length) of thymocytes migrating towards SDF-1 releasing beads by more than 20 μm (Figure 5d). Although directionality index was not altered significantly between WT and GIT2$^{-/-}$ thymocytes (Figure 5d, *left panel*), there were more GIT2$^{-/-}$ thymocytes migrating in the velocity range between 4–6 μm/min (Figure 5d, *right panel*). From these results, we conclude that GIT2 deficiency increases SDF-1-induced motility.

GIT2 deficiency promotes Rac1 activation and actin polymerization following SDF-1 or CCL25 stimulation

The small GTPase Rac is activated in response to SDF-1 and is thought to play a critical role in cytoskeletal reorganization events that govern cell migration. Although we found TCR-induced Rac activation was not changed in GIT2$^{-/-}$ thymocytes, we thought that SDF-1-induced Rac activation might be affected in the absence of GIT2 since we saw increased migration in GIT2$^{-/-}$ thymocytes in response to SDF-1. Indeed, Rac1 activation response of GIT2$^{-/-}$ thymocytes to SDF-1 was consistently increased compared to WT thymocytes suggesting that negative regulation of Rac1 activation by GIT2 is specific to chemokine receptor stimulation (Fig. 6a). Next, we examined actin polymerization in response to SDF-1. SDF-1 treatment of WT thymocytes increased total polymerized actin transiently (Fig. 6b). The increase in the amount of polymerized actin was greater at all time points in

GIT2$^{-/-}$ DP and CD4 SP thymocytes. We also found that CCL25 stimulation transiently induced Rac1 activation and actin polymerization in WT thymocytes and both responses were increased in GIT2$^{-/-}$ thymocytes similar to SDF-1 stimulation (data not shown). The PAK2-α/β PIX interaction and PAK2 kinase activity in response to SDF-1 was normal in the absence of GIT2 (Supplementary Figure 5d, 5e). Collectively, these data indicate that Rac1 activation and actin polymerization in response to SDF-1 or CCL25 are increased in the absence of GIT2. This hyper-activation is likely to contribute to the increased migratory response of GIT2$^{-/-}$ thymocytes.

Although it is weak, SDF-1 also induces ERK activation in DP thymocytes. Since positive selection is dependent on Erk activation, we examined ERK activation following SDF-1 stimulation and did not find substantial differences between WT and GIT2$^{-/-}$ DP thymocytes (Supplementary Fig. 4a for OTII; data not shown for DO11.10). These results indicate that GIT2 affects pathways leading to Rac activation (and actin polymerization) specifically but not those leading to ERK activation following SDF-1 stimulation.

SDF-1- and CCL25-induced migration of TCR transgenic GIT2$^{-/-}$ thymocytes is increased

Because chemotaxis of GIT2$^{-/-}$ DP thymocytes with a diverse repertoire was greatly enhanced in response to SDF-1 and CCL25, it is likely that the responses of TCR transgenic GIT2$^{-/-}$ DP thymocytes to these chemokines are also increased. Indeed, we found that is the case (Supplementary Fig. 8a, *left panel*). Like non-transgenic GIT2$^{-/-}$ mice, chemotaxis of GIT2$^{-/-}$ pre-selection DP thymocytes (TCR transgene^{low}) was enhanced more than post-selection DP thymocytes (TCR transgene^{hi}) (Supplementary Fig. 8a, *middle and right panels*). We also examined thymocyte migration under competitive conditions. By mixing TCR transgenic WT or GIT2$^{-/-}$ thymocytes with two different congenic markers, each population could be tracked. We found that even under these competitive conditions, TCR transgenic GIT2$^{-/-}$ DP thymocytes displayed enhanced migration in response to SDF-1 and CCL25 than GIT2-sufficient cells (Supplementary Fig. 8b).

More GIT2$^{-/-}$ DP thymocytes migrate towards chemokines even when TCR-mediated stop signal is present

Previous reports have shown that effector T cells from TCR transgenic mice migrate vigorously on adhesion molecule ICAM-1-coated surfaces, but stop migrating when their TCR is stimulated by an appropriate pMHC molecule[37]. Likewise, DP thymocytes randomly migrate in the thymus in search of a pMHC ligand for their newly formed TCR but pMHC ligation of the TCR leads to a stop signal prolonging the duration of thymocyte-stromal interactions, from which selection decisions can be determined[2–4]. Since loss of GIT2 results in increased migration of DP thymocytes in response to chemokines that are expressed in the cortex, we asked whether the increased chemotactic activity of GIT2$^{-/-}$ thymocytes interferes with the TCR-mediated stop signal. To examine this, we adapted an experimental system described previously[38], in which a TCR-mediated stop signal and a chemokine-induced migratory signal co-exist on the top filter of a transwell system. Since TCR transgenic GIT2$^{-/-}$ thymocytes express a reduced level of surface TCR, we used non-transgenic GIT2$^{-/-}$ mice that express similar level of CD3 compared to WT cells. When control BSA-coated filters were used, as we described above, the migration of GIT2$^{-/-}$ DP thymocytes was substantially increased in response to SDF-1 (Fig. 7a). When ICAM-1 coated filters were used in the presence of SDF-1, migration of both WT and GIT2$^{-/-}$ thymocytes was greatly increased, suggesting that presence of ICAM-1 facilitates transwell migration in response to SDF-1. When ICAM-1 plus CD3 coated filters were used in the presence of SDF-1 (Fig. 7b), the migration of WT DP thymocytes was markedly reduced suggesting that the TCR-mediated stop signal is effective even though a chemotactic signal is simultaneously present. The TCR-mediated stop signal is also dose dependent, since a

higher concentration of CD3 induced a more efficient block in migration. In GIT2$^{-/-}$ DP thymocytes, the effect of the TCR-mediated stop signal upon SDF1- mediated migration was less potent. For instance, at a higher dose of CD3 with ICAM-1, 25% of input GIT2 $^{-/-}$ DP thymocytes migrated in response to SDF-1 resulting in a 2.5-fold increase in migration compared to WT DP cells. These results indicate that although the TCR-mediated stop signal can inhibit SDF-1-mediated migration in both WT and GIT2$^{-/-}$ DP thymocytes, more GIT2$^{-/-}$ DP thymocytes can overcome a TCR-mediated stop signal, allowing them to migrate to SDF-1. Thus, we conclude that the increased chemotactic activity of GIT2$^{-/-}$ DP thymocytes is likely to compromise a TCR-induced stop signal in DP thymocytes.

Scanning activity of GIT2$^{-/-}$ thymocytes in the cortex is severely impaired

To determine whether GIT2 deficiency affects T cell migration in intact thymic lobes, we set up an experimental system in which the migration of WT and GIT2$^{-/-}$ thymocytes is monitored in the same thymic environment using two photon laser scanning microscopy (TPLSM) (Figure 8a). Bone marrow cells from GIT2$^{-/-}$ mice expressing a GFP transgene under the control of the ubiquitin promoter (UBI-GFP) and WT mice expressing a CFP transgene under the control of the actin promoter (Actin-CFP) were mixed with WT non-fluorescent bone marrow cells and then transferred into irradiated hosts to generate partial hematopoietic chimeras in which approximately 1% of thymocytes are derived from either the GFP-or CFP- expressing donor. After 6–8 weeks, intact thymic lobes from adult chimeric mice were explanted, and migratory behaviors of thymocytes were monitored using TPLSM 30–90 μm under the thymic capsule, an analysis that is limited to the cortex and can not image the medulla or corticomedullary junction. In contrast to WT thymocytes that randomly migrated in the cortex (4.74 μm/min), GIT2$^{-/-}$ thymocytes displayed markedly decreased motility (2.85 μm/min) (Figure 8b, 8c, Supplementary movie 2). The GIT2$^{-/-}$ thymocytes accumulated at discrete small regions throughout the cortex including areas close to small blood vessels and tended to circle around to their place of origin, in marked contrast to the behavior of WT thymocytes that tended to migrate more distally. To quantify this difference in behavior we calculated the directionality index (displacement divided by path length) for individual thymocytes. While the directionality index tends to increase with speed for wild type thymocytes, this was not the case for GIT2$^{-/-}$ thymocytes (Figure 8d). As a result, the directionality indices of WT cells that migrated with average speeds between two and five μm/min were significantly increased compared to GIT2$^{-/-}$ thymocytes of equivalent speed (***: P=0.0004 for 2–3 μm/min speeds; ***: P<0.0001 for 3–4 μm/min speeds; ***: P<0.0001 for 4–5 μm/min speeds). One possible explanation for the altered migration of GIT2$^{-/-}$ thymocytes *in vivo* is that hypersensitivity to chemokines leads to trapping of thymocytes near local sources of chemokines in the cortex. Indeed, it was recently reported that SDF-1 is present at scattered sites in the cortex, including associated with small blood vessels[39], an observation that we confirm here (Figure 8f). Furthermore, some GIT2$^{-/-}$ thymocytes interacted extensively with small blood vessels in the cortex, moving back and forth along their surfaces (Figure 8e, Supplementary movie 3) rather than moving away from blood vessels likd WT thymocytes (Supplementary movie 4). The major function of small blood vessels in the cortex is likely to deliver oxygen or nutrients, rather than to serve as entry or exit portals for thymocytes, a function of post capillary venules (PCV) at the corticomedullary junction and in the adjacent medulla[40]. Thus, interaction of thymocytes with small blood vessels in the cortex is not likely to represent thymocyte entering or exiting behavior. Furthermore, we did not find any evidence suggesting increased thymic entry or impaired exit, for example, increased T cells in blood or accumulation of CD4 or CD8 SP cells in the thymus.

Together, these data suggest that, in the absence of GIT2, cortical thymocytes react too strongly to local chemokine gradients, thereby preventing them from efficiently scanning

cortical epithelial cells, and leading to impaired positive selection. Indeed, we found a very small population of fast-migrating WT thymocytes at higher than 13 μm/min motility rates that likely represent DP thymocytes at a later stage of positive-selection but did not observe such high speeds in GIT2$^{-/-}$ thymocytes, suggesting decreased numbers of late-stage positively selected GIT2$^{-/-}$ thymocytes.

Discussion

We report that GIT2 negatively regulates DP thymocyte migration in response to SDF-1 and CCL25, chemokines that play critical roles in the thymus. In the absence of GIT2, *in vitro* migration of DP thymocytes to these chemokines was greatly increased. Moreover, SDF-1-induced Rac activation and actin polymerization was substantially increased in GIT2$^{-/-}$ thymocytes, suggesting GIT2 represses chemokine-induced migration via a mechanism that involves disrupted Rac activation and actin polymerization. Intriguingly, the scanning activity of GIT2$^{-/-}$ thymocytes in intact thymic lobes was severely compromised due to decreased motility. We propose that the *in vivo* migration defect of the GIT2$^{-/-}$ thymocytes is due to inappropriate responses to local chemokine gradients, causing thymocytes to be trapped near sources of chemokines in the cortex and preventing them from efficiently scanning thymic epithelial cells during positive selection. Indeed, we found that a subpopulation of GIT2$^{-/-}$ thymocytes intensively interacted with small blood vessels, which are often surrounded by SDF-1 positive cells. The impaired scanning activity of GIT2$^{-/-}$ thymocytes, without detectable downstream biochemical changes in ERK activation and Ca^{2+} mobilization, was accompanied by impaired positive selection in TCR transgenic GIT2$^{-/-}$ mice, suggesting there is a relationship between thymocyte motility and positive selection.

It is intriguing that although the *in vitro* motility of GIT2$^{-/-}$ thymocytes to chemokines was increased (Figure 4 and 5), *in vivo* motility of GIT2$^{-/-}$ thymocytes within thymic lobes was reduced (Figure 8c). Because the intrinsic migratory ability of GIT2$^{-/-}$ thymocytes is intact and even increased compared with WT thymocytes *in vitro*, it is unlikely that *in vivo* migratory behavior reflects the different developmental stages of GIT2$^{-/-}$ thymocytes. We hypothesize that the increased responsiveness of GIT2$^{-/-}$ thymocytes to chemokines leads to an enhanced steady state interaction with local chemokine sources, independent of TCR-pMHC interaction. Hypersensitivity of GIT2$^{-/-}$ thymocytes to a chemokine signals could result in their inability to reprioritize other guidance cues present in cortical epithelial cells that facilitate TCR-pMHC interaction, and instead leads to a maintenance of interactions with chemokine expressing sources such as small blood vessels. This could ultimately prevent them from sampling multiple cTECs in search of pMHC with the right range of affinity and avidity, thereby leading to inefficient positive selection.

Although *in vitro* experiments clearly indicate enhanced responsiveness of GIT2$^{-/-}$ thymocytes to chemokines (Figure 4 and 5), we did not observe greater accumulation of GIT2$^{-/-}$ DP thymocytes near SDF-1-releasing alginate beads (Supplemental Figure 7 and Supplemental Movie 1) as we did *in vivo* using TPLSM (Figure 8). There could be several explanations for this. For instance, the *in vivo* thymic environment is more complex than the *in vitro* one. Adhesion molecules such as integrins as well as others could promote stable interactions of thymocytes. In contrast, such adhesion molecules are not present on the SDF-1-releasing beads in the *in vitro* system. In addition, multiple SDF-1 releasing beads were added to facilitate locating them in the imaging field, each of which can generate a separate gradients in the same assay environment, which could distract cells. Furthermore, it may require significantly more time to see more accumulation of GIT2 $^{-/-}$ thymocytes near the chemokine source *in vitro*. In contrast, the *in vivo* using TPLSM system reflects the

steady-state consequence of long-lasting physiological interactions between GIT2−/− thymocytes and local chemokine sources after 6–8 weeks of thymic repopulation.

Unlike GIT2$^{-/-}$ thymocytes that were able to sense SDF-1 and migrate toward it (Supplemental Figure 7 and Supplemental Movie 1), GIT2$^{-/-}$ neutrophils have been reported to exhibit defects in sensing the chemo-attractant fMLP[27]. The basis for this difference may be due to the utilization of the fMLP receptor of the Gβγ-PAK1-αPIX-GIT2 signaling machinery exclusively for directional sensing. It is possible that CXCR4 in thymocytes utilizes different signaling machinery for sensing direction, but utilizes GIT2 for other process, for example regulating Rac activation and actin polymerization, as we demonstrated (Figure 6). Indeed, GIT2 deficiency in neutrophils impaired PAK1 activation following fMLP stimulation; however GIT2 deficiency in the thymocytes did not affect PAK2 activation or PAK2-PIX interaction following SDF-1 stimulation.

It is unclear why the pre-selection GIT2$^{-/-}$ DP thymocytes show the most exaggerated migration responses to SDF-1 or CCL25. One possibility is that GIT2 protein is more abundant in the pre-selection DP thymocytes. However, GIT2 mRNA levels in sorted CD69^{low} and CD69^{hi} DP populations were similar (data not shown). Another possibility is that GIT2 is a limiting factor in the pre-selection stage to suppress chemotactic ability but following positive selection, other regulators of chemotaxis are expressed, partially compensating for GIT2 deficiency. Identification of negative regulators of chemokine-induced migration at different developmental stages would clarify the regulation of thymocyte migration during development.

Although our results indicate that GIT2 suppresses Rac activation following SDF-1- or CCL25- stimulation, the mechanism by which GIT2 negatively regulates Rac activation requires further investigation. Because Arf6 can activate Rac[21], GIT2 may inhibit Rac activation by negatively regulating Arf6 via its GAP activity. However, we did not detect any increase in an active form of Arf6 in basal- or SDF-1- stimulation conditions in WT and GIT2$^{-/-}$ thymocytes using a biochemical pull-down assay (data not shown). Although this may be explained by the limited sensitivity of this assay, it is also possible that GIT2-mediated Rac suppression may be independent of the Arf GAP activity of GIT2. Further studies will be needed to clarify the mechanism of GIT2-mediated repression of Rac activation.

Inhibition of negative regulators of cell migration may enhance the recruitment of antigen-reactive or autoreactive cells to the inflamed tissues. GIT2 was initially identified by its interaction with GPCR kinases including GRK2[22]. Interestingly, in peripheral T cells, a 50% reduction of in GRK2 level in GRK2+/− mice correlates with a substantial increase in chemokine-induced migration, suggesting a role of GRK2 in inhibiting chemokine-induced cell migration[41]. Interestingly, expression of GRK2 is reduced by 50% in peripheral blood mononuclear cells of patients with rheumatoid arthritis[42] and multiple scelerosis[43]. Thus, it will be of interest to determine whether loss of GIT2 potentiates SDF-1- mediated recruitment of antigen-responsive or autoreactive T cells to the inflamed tissues in models of rheumatoid arthritis or multiple sclerosis. The development of reagents that control the function of GIT2 or other negative regulators of migration may be a valuable strategy for novel therapeutics that target the immune system.

Methods

Antibodies and reagents

Antibodies to murine CD1d, CD3, CD4, CD5, CD8, CD11b, CD19. CD21, CD23, CD44, CD62L, CD69, Gr-1, IgD, IgM, Vβ3, Vβ5, Vβ8, Vβ11or B220 conjugated to FITC, PE,

PerCP-Cy5.5, PE-Cy7, Pacific Blue, allophycocyanin, or Alexa Fluor 647 were obtained from eBioscience or BD Biosciences. Active caspase 3 for intracellular staining was purchased from BD Biosciences. Erk1 and 2 Abs for western blotting analysis were obtained from Santa Cruz Biotechnology. Phospho-Erk Abs used for Western blotting and flow cytometry were obtained from Cell Signaling. The anti-PAK1, PAK2, SDF-1 antibodies, sc881, sc1872, and sc-6193, were obtained from Santa Cruz Biotechnology. The anti-PIX antibody was described previously[44] and was provided by Dr. Manser (Glaxo-IMCB Group, Institute of Molecular and Cell Biology, Singapore). Stimulatory armenian hamster anti-mouse CD3ε (clone name: 2C11) antibody was produced and purified using standard methods. Goat anti-Armenian hamster IgG (H and L chains) Abs and goat anti-rabbit IgG Abs conjugated to either PE or allophycocyanin were obtained from Jackson ImmunoResearch Laboratories.

Flow cytometry

Single cell suspensions were prepared from thymi, lymph nodes (LN) and spleens. Fc receptors were blocked with rat anti-CD16/32 (clone 2.4G2; BD Biosciences). Ten million cells were stained with the indicated Abs and analyzed on a FACSCalibur (BD Biosciences) or a CyAN ADP (Beckman Coulter) flow cytometry system. Forward and side scatter exclusion was used to identify live cells. Data analysis was performed using FlowJo (version 8.8.4) software (Tree Star).

In vivo BrdU incorporation assay

For in vivo BrdU labeling studies, each mouse received a single i.p. injection with 2 mg BrdU (BD Biosciences) at 20 mg/ml and was maintained on drinking water supplemented with 0.8 mg/ml BrdU (Sigma-Aldrich) with 2% glucose added to the water for up to 2 d. Data points for BrdU+ CD4+CD8+ DP or CD4 and CD8 SP thymocytes are shown as a percentage of total thymocytes. Staining for BrdU positive cells was performed according to the manufacturer's instruction (BD Biosciences).

Detection of apoptotic or dead cells

Annexin V-FITC or Annexin V-PE Apoptosis Detection Kits (BD Biosciences) were used for detection of apoptotic and dead cells. Single-cell suspensions of thymus were washed twice with PBS before resuspension in the provided buffer and incubation with CD4, CD8, annexin V and 7AAD. Cells were subsequently analyzed by flow cytometry. For intracellular staining of active caspase 3, single cell suspension of thymocytes was stained with CD4 and CD8, washed in FACS buffer. Cells were fixed and permeabilized using the BD Cytofix/Cytoperm™ Kit (BD Biosciences) and stained with anti-active caspase 3 antibody (BD Biosciences) for 1 hour following the manufacturer's instruction and analyzed for flow cytometry.

Competitive repopulation experiments and bone marrow chimera

For DO11.10+WT or DO11.10+GIT2$^{-/-}$ adoptive transfers, bone marrow cells from DO11.10+WT or DO11.10+GIT2$^{-/-}$ mice were harvested, resuspended in 1.0 ml (10^7 cells/ml) PBS and 200 μl (2×10^6 bone marrow cells) was injected i.v. into lethally irradiated BALB/c recipients. BALB/c recipients were irradiated with two doses of 600 rads, 3–5 h apart. After 6–8 weeks, thymi of reconstituted chimeras were harvested and used for FACS analysis.

For mixed bone marrow (BM) chimera experiments, BM chimeras were generated by transfering 1:1 mixed BM cells from OTII+ WT (CD45.1/CD45.2) and OTII+ GIT2$^{-/-}$ mice (CD45.2/CD45.2) with different congenic markers into lethally irradiated BoyJ recipients

(CD45.1/CD45.1). BoyJ recipients were irradiated with two doses of 600 rads, 3–5 h apart. Mixed BM cells were resuspended in 1.0 ml (10^7 cells/ml) PBS and 200 μl (2×10^6 mixed bone marrow cells) was injected i.v. into each mouse. Thymus, spleen, lymph nodes and blood from reconstituted animals were analyzed 8 wk later.

Transwell migration assay

The migratory ability of T cells was measured using 5 μm pore size Transwell plates (Corning Costar Corp). Briefly, for thymocyte migration assays, 10^7 thymocytes were resuspended in 1.0 ml of migration buffer (0.5% BSA, 10mM HEPES, RPMI 1640) and incubated for 10 min at 37°C. Cells were allowed to migrate across 5 μm transwell filter to the bottom chamber containing 600 μl of either migration buffer alone (media) or with various chemokines (R&D systems) for 3 hours. Cells were collected, stained with anti-CD4, CD8, CD69, TCRβ or CD3, and quantified using flow cytometry. Migration of distinct populations is presented as a percent of migrating cell number divided by input cell number. Transwell assays were performed in duplicates for each different chemokine (SDF-1, 400 ng/ml; CCL25, 2.5 μg/ml; CCL19, 250 ng/ml and CCL21, 1 μg/ml). For transwell migration assays using filters coated with ICAM-1 or ICAM-1 plus anti-CD3, 5μm polycarbonate transwell filters were coated in 100 μl of PBS with ICAM-1 (R&D systems, 3 μg/ml) or ICAM-1 plus CD3 (2C11, 5 μg/ml or 20 μg/ml) overnight at 4°C. Filters were washed three times with PBS and blocked with 2% BSA for 1 hour at 37°C. Filters were then washed three times with PBS and dried completely for 2 hours. Coated filters were checked for leakage, then used for transwell migration assays as described above.

Rac1 activation assay

Specific isolation of Rac1-GTP was performed as described previously[45, 46]. Thymocytes were harvested in migration buffer (0.5% BSA, 10mM HEPES, RPMI 1640), single cell suspensions were prepared, and then incubated in migration buffer at 37°C for 30 min. Twenty to thirty million thymocytes were stimulated with 400 ng/ml of SDF-1 or 2.5 μg/ml of CCL21, then lysed immediately in ice-cold 2x lysis buffer (50 mM HEPES (pH 7.5), 300 mM NaCl, 2% NP-40, 20% Glycerol, 50 mM NaF, 20 mM $MgCL_2$, 2 mM EDTA, 2 mM sodium orthovanadate, 20 μg/ml Leupeptin, 20 μg/ml Aprotinin). The lysates were cleared by centrifugation at 16,000 g for 3 minutes, and transferred into microfuge tubes that contained 10 μl of PAK1-PBD agarose (Upstate Biotechnology). After 20 minutes of tumbling at 4°C, lysates with PAK1-PBD agarose were briefly centrifuged and transferred to Micro Bio-Spin Columns (Bio-Rad). PAK1-PBD agarose-bound material in the column was washed twice with 0.5 ml of ice-cold lysis buffer. Columns with PAK1-PBD agarose bound materials were centrifuged to remove excess liquid. The PAK1-PBD-bound proteins were eluted by adding 30 μl of preheated 2X sample buffer and were subjected to SDS-PAGE using precast 4%–12% gradient gels (Invitrogen). Rac1 protein was detected by western blot analysis as previously described[30].

Actin polymerization assay

Thymocytes were harvested in migration media (0.5% BSA, 100mM HEPES in RPMI 1640). Single cell suspensions of thymocytes were counted, resuspended to 20 x 10^6/ml in the same media and rested for 30 min. One million thymocytes were stimulated with SDF-1 (final concentration 400 ng/ml) for various times and then fixed with an equal volume of Cell Fixative (BD Biosciences) for 10 min. Cells were washed twice with PBS, permeabilized in 0.1% Triton X-100 for 5 min, and washed twice with PBS. Cells were stained with 100 μl of PBS containing 2.5 μl of Alexa-488 conjugated phalloidin, CD4-Alexa647 and CD8-PercpCy5.5 for 20 min. Cells were washed twice and subjected to flow

cytometry. CD4+CD8+ DP thymocytes and CD4 SP thymocytes were gated and mean fluorescence intensity was measured using FlowJo software.

Migration assays

WT or GIT2$^{-/-}$ thymocytes were harvested in RPMI media supplemented with 2% FBS and 10 mM HEPES and labeled separately with 0.2 μM of CFSE ((5-(and-6)-carboxyfluorescein diacetate, succinimidyl ester) or 2 μM of CMTMR (5(and-6)-(((4-chloro-methyl) benzoyl) amino) tetramethylrhodamine)(Invitrogen). Labeled thymocytes were mixed at 2×10^6 cells/ml in RPMI media supplemented with 2% FBS and 10 mM HEPES. Migration assays on two-dimensional surfaces were performed by plating a mixture of 1×10^5 WT and GIT2$^{-/-}$ thymocytes in chambered coverglasses (Lab-Tek) and adding low melting-point agarose to a final concentration of 0.1%. Migration in collagen lattices was performed in a 1.5 mg/ml collagen solution in RPMI supplemented 2% FBS, 10 mM HEPES and 300 alginate beads. Alginate beads were synthesized as previously described[36]. SDF-1 (1 μg) was incubated with 3×10^4 of alginate beads for 1 hour at 4°C, washed, and resuspended in 100 μl of RPMI supplemented 2% FBS, 10 mM HEPES. Three hundred non-loaded or SDF-1 loaded alginate beads were mixed with the collagen solution containing thymocytes, transferred to chambered coverglass, briefly centrifuged in 1000 RPM for 3 min, and immediately imaged. Wide-field imaging for migration assays was performed on a modified Axiovert 200M microscope (Zeiss) with a 20×/0.75 NA objective and a Coolsnap HQ camera (Roper Scientific). The wide-field microscope was equipped with dual excitationand emission filter wheels and the control and imaging software was Metamorph (Universal Imaging Corp.). All microscopes were configured with heated stages to maintain sample temperature at 37°C. For analysis, cell viability was assessed using the bright field images while cell movement was measured based on the center of mass of GFP or CMTMR fluorescence using Imaris tracking software (Bitplane). For measuring average speeds, cells that appeared in the field for more than 500 sec and that had a displacement of more than 20 μm were selected and analyzed. For directionality index, thymocytes migrating towards SDF-1 releasing beads by more than 20 μm were selected and analyzed.

Two-photon imaging

Six to eight weeks after the bone marrow transfer, the GIT2$^{-/-}$ GFP chimeric mice were injected through the tail vein with 250 μg of Tomato lectin (Vector laboratories) conjugated to Alexa Fluor 594 2 min before sacrifice. Intact thymic lobes were cleaned carefully from the surrounding connective tissue, glued to a cover slip and imaged by two-photon laser scanning microscopy while being perfused with warmed, oxygenated DMEM without phenol red medium. Imaging volumes of 172 × 143 × 40–60 μm were scanned every 30 sec for 20 min with a custom-built microscope with a Spectra-Physics Mai-Tai laser tuned to 880 nm for excitation of CFP, GFP and Alexa Fluor 594. The emitted light was separated with 495 nm and 560 nm dichroic mirrors and passed through 450/80 nm, 525/50 nm and 645/75 nm band-pass filters (Chroma). Imaging volumes were at least 30 μm under the capsule.

Data analysis

The x, y, z coordinates of individual thymocytes over time were obtained with Imaris 5.7.2 software (Bitplane). The data were graphed with Prism (GraphPad).

Immunofluorescence and blood vessel labeling

To label vasculature, mice were injected via tail vein with 100 μg of tomato lectin-FITC (Vector Laboratories) just before sacrifice. Isolated thymic lobes were fixed in 4% formalin and 10% sucrosefor 1 h, sequentially submerged in 10, 20, and 30% sucrose for 10–18 h

each, and frozen over dry ice in OCT. Sections, 7 mm thick, were cut with a Leica CM 3050S cryomicrotome (Leica Microsystems). Sections were fixed with cold acetone for 10 min, blocked with 10% donkey serum in PBS for an hour, stained with anti-SDF-1 at a 1:50 dilution of 0.2 mg/ml stock (Santa Cruz) for three hours at 4°C, and stained with donkey anti-goat Alexa 588 conjugate (Invitrogen) for 1 hour at room temperature. Negative controls consisted of pre-absorbing the SDF-1 antibody (4 mg/ml) with 2 mg/ml of recombinant murine SDF-1 (R&D Systems) at 37°C for 1 hour prior to use or leaving off the primary antibody. Stained thymic sections were visualized on a Nikon Eclipse E800 fluorescence microscope equipped with SimplePCI software (Compix). Images were converted to red-green, colored and overlaid with Adobe Photoshop CS2 software (Adobe Systems). For 40x magnification, confocal imaging was acquired using a modified Axiovert 200M microscope equipped with a spinning-disk confocal scanner (Yokogawa) with a 40x/1.3NA oil immersion objective.

Supplementary Material

Refer to Web version on PubMed Central for supplementary material.

Acknowledgments

We thank the UCSF Comprehensive Cancer Center Transgenic/TargetedMutagenesis Core Facility for creating the GIT2$^{-/-}$ mice; Jason Cyster, Nigel Kileen, Andre Limnander and Byron Au-Yeung for reading this manuscript and for helpful comments; the Biological imaging Development Center at UCSF for Imaris software support; and Matthew F. Krummel and Jordan Jacobelli for confocal and time lapse fluorescence microscopy support. We would also like to thank Al Roque for assistance with animal husbandry and membersof the Weiss Laboratory for helpful discussions. H.P. was supported, in part, by a Leukemia and Lymphoma Society Special Fellow Award.

References

1. Ladi E, Yin X, Chtanova T, Robey EA. Thymic microenvironments for T cell differentiation and selection. Nature immunology. 2006; 7:338–343. [PubMed: 16550196]
2. Bousso P, Bhakta NR, Lewis RS, Robey E. Dynamics of thymocyte-stromal cell interactions visualized by two-photon microscopy. Science (New York, NY. 2002; 296:1876–1880.
3. Witt CM, Raychaudhuri S, Schaefer B, Chakraborty AK, Robey EA. Directed migration of positively selected thymocytes visualized in real time. PLoS biology. 2005; 3:e160. [PubMed: 15869324]
4. Bhakta NR, Oh DY, Lewis RS. Calcium oscillations regulate thymocyte motility during positive selection in the three-dimensional thymic environment. Nature immunology. 2005; 6:143–151. [PubMed: 15654342]
5. Ladi E, et al. Thymocyte-dendritic cell interactions near sources of CCR7 ligands in the thymic cortex. J Immunol. 2008; 181:7014–7023. [PubMed: 18981121]
6. Suzuki G, et al. Pertussis toxin-sensitive signal controls the trafficking of thymocytes across the corticomedullary junction in the thymus. J Immunol. 1999; 162:5981–5985. [PubMed: 10229836]
7. Zaitseva MB, et al. CXCR4 and CCR5 on human thymocytes: biological function and role in HIV-1 infection. J Immunol. 1998; 161:3103–3113. [PubMed: 9743377]
8. Wurbel MA, et al. The chemokine TECK is expressed by thymic and intestinal epithelial cells and attracts double- and single-positive thymocytes expressing the TECK receptor CCR9. Eur J Immunol. 2000; 30:262–271. [PubMed: 10602049]
9. Misslitz A, et al. Thymic T cell development and progenitor localization depend on CCR7. The Journal of experimental medicine. 2004; 200:481–491. [PubMed: 15302903]
10. Uehara S, Song K, Farber JM, Love PE. Characterization of CCR9 expression and CCL25/thymus-expressed chemokine responsiveness during T cell development: CD3(high)CD69+ thymocytes and gammadeltaTCR+ thymocytes preferentially respond to CCL25. J Immunol. 2002; 168:134–142. [PubMed: 11751956]

11. Choi YI, et al. PlexinD1 glycoprotein controls migration of positively selected thymocytes into the medulla. Immunity. 2008; 29:888–898. [PubMed: 19027330]
12. Turner CE. Paxillin interactions. J Cell Sci. 2000; 113(Pt 23):4139–4140. [PubMed: 11069756]
13. Frank SR, Hansen SH. The PIX-GIT complex: a G protein signaling cassette in control of cell shape. Semin Cell Dev Biol. 2008; 19:234–244. [PubMed: 18299239]
14. Randazzo PA, Inoue H, Bharti S. Arf GAPs as regulators of the actin cytoskeleton. Biol Cell. 2007; 99:583–600. [PubMed: 17868031]
15. Hoefen RJ, Berk BC. The multifunctional GIT family of proteins. J Cell Sci. 2006; 119:1469–1475. [PubMed: 16598076]
16. Sabe H, Onodera Y, Mazaki Y, Hashimoto S. ArfGAP family proteins in cell adhesion, migration and tumor invasion. Curr Opin Cell Biol. 2006; 18:558–564. [PubMed: 16904307]
17. Vitale N, et al. GIT proteins, A novel family of phosphatidylinositol 3,4, 5-trisphosphate-stimulated GTPase-activating proteins for ARF6. The Journal of biological chemistry. 2000; 275:13901–13906. [PubMed: 10788515]
18. Premont RT, Claing A, Vitale N, Perry SJ, Lefkowitz RJ. The GIT family of ADP-ribosylation factor GTPase-activating proteins. Functional diversity of GIT2 through alternative splicing. The Journal of biological chemistry. 2000; 275:22373–22380. [PubMed: 10896954]
19. Radhakrishna H, Al-Awar O, Khachikian Z, Donaldson JG. ARF6 requirement for Rac ruffling suggests a role for membrane trafficking in cortical actin rearrangements. J Cell Sci. 1999; 112 (Pt 6):855–866. [PubMed: 10036235]
20. D'Souza-Schorey C, Chavrier P. ARF proteins: roles in membrane traffic and beyond. Nat Rev Mol Cell Biol. 2006; 7:347–358. [PubMed: 16633337]
21. Santy LC, Casanova JE. Activation of ARF6 by ARNO stimulates epithelial cell migration through downstream activation of both Rac1 and phospholipase D. J Cell Biol. 2001; 154:599–610. [PubMed: 11481345]
22. Premont RT, et al. beta2-Adrenergic receptor regulation by GIT1, a G protein-coupled receptor kinase-associated ADP ribosylation factor GTPase-activating protein. Proceedings of the National Academy of Sciences of the United States of America. 1998; 95:14082–14087. [PubMed: 9826657]
23. Bagrodia S, et al. A tyrosine-phosphorylated protein that binds to an important regulatory region on the cool family of p21-activated kinase-binding proteins. The Journal of biological chemistry. 1999; 274:22393–22400. [PubMed: 10428811]
24. Turner CE, et al. Paxillin LD4 motif binds PAK and PIX through a novel 95-kD ankyrin repeat, ARF-GAP protein: A role in cytoskeletal remodeling. J Cell Biol. 1999; 145:851–863. [PubMed: 10330411]
25. Frank SR, Adelstein MR, Hansen SH. GIT2 represses Crk- and Rac1-regulated cell spreading and Cdc42-mediated focal adhesion turnover. Embo J. 2006; 25:1848–1859. [PubMed: 16628223]
26. Zhang H, Webb DJ, Asmussen H, Niu S, Horwitz AF. A GIT1/PIX/Rac/PAK signaling module regulates spine morphogenesis and synapse formation through MLC. J Neurosci. 2005; 25:3379–3388. [PubMed: 15800193]
27. Mazaki Y, et al. Neutrophil direction sensing and superoxide production linked by the GTPase-activating protein GIT2. Nature immunology. 2006; 7:724–731. [PubMed: 16715100]
28. Nishiya N, Kiosses WB, Han J, Ginsberg MH. An alpha4 integrin-paxillin-Arf-GAP complex restricts Rac activation to the leading edge of migrating cells. Nat Cell Biol. 2005; 7:343–352. [PubMed: 15793570]
29. Ku GM, Yablonski D, Manser E, Lim L, Weiss A. A PAK1-PIX-PKL complex is activated by the T-cell receptor independent of Nck, Slp-76 and LAT. Embo J. 2001; 20:457–465. [PubMed: 11157752]
30. Phee H, Abraham RT, Weiss A. Dynamic recruitment of PAK1 to the immunological synapse is mediated by PIX independently of SLP-76 and Vav1. Nature immunology. 2005; 6:608–617. [PubMed: 15864311]
31. Schmalzigaug R, Phee H, Davidson CE, Weiss A, Premont RT. Differential expression of the ARF GAP genes GIT1 and GIT2 in mouse tissues. J Histochem Cytochem. 2007; 55:1039–1048. [PubMed: 17565117]

32. Kisielow P, Bluthmann H, Staerz UD, Steinmetz M, von Boehmer H. Tolerance in T-cell-receptor transgenic mice involves deletion of nonmature CD4+8+ thymocytes. Nature. 1988; 333:742–746. [PubMed: 3260350]
33. Kisielow P, Teh HS, Bluthmann H, von Boehmer H. Positive selection of antigen-specific T cells in thymus by restricting MHC molecules. Nature. 1988; 335:730–733. [PubMed: 3262831]
34. Azzam HS, et al. CD5 expression is developmentally regulated by T cell receptor (TCR) signals and TCR avidity. The Journal of experimental medicine. 1998; 188:2301–2311. [PubMed: 9858516]
35. Campbell JJ, Pan J, Butcher EC. Cutting edge: developmental switches in chemokine responses during T cell maturation. J Immunol. 1999; 163:2353–2357. [PubMed: 10452965]
36. Hori Y, Winans AM, Huang CC, Horrigan EM, Irvine DJ. Injectable dendritic cell-carrying alginate gels for immunization and immunotherapy. Biomaterials. 2008; 29:3671–3682. [PubMed: 18565578]
37. Dustin ML, Bromley SK, Kan Z, Peterson DA, Unanue ER. Antigen receptor engagement delivers a stop signal to migrating T lymphocytes. Proceedings of the National Academy of Sciences of the United States of America. 1997; 94:3909–3913. [PubMed: 9108078]
38. Bromley SK, Peterson DA, Gunn MD, Dustin ML. Cutting edge: hierarchy of chemokine receptor and TCR signals regulating T cell migration and proliferation. J Immunol. 2000; 165:15–19. [PubMed: 10861029]
39. Trampont PC, et al. CXCR4 acts as a costimulator during thymic beta-selection. Nature immunology. 2010; 11:162–170. [PubMed: 20010845]
40. Kato S. Thymic microvascular system. Microscopy research and technique. 1997; 38:287–299. [PubMed: 9264340]
41. Vroon A, et al. Reduced GRK2 level in T cells potentiates chemotaxis and signaling in response to CCL4. J Leukoc Biol. 2004; 75:901–909. [PubMed: 14761932]
42. Lombardi MS, et al. Decreased expression and activity of G-protein-coupled receptor kinases in peripheral blood mononuclear cells of patients with rheumatoid arthritis. Faseb J. 1999; 13:715–725. [PubMed: 10094932]
43. Vroon A, et al. G protein-coupled receptor kinase 2 in multiple sclerosis and experimental autoimmune encephalomyelitis. J Immunol. 2005; 174:4400–4406. [PubMed: 15778405]
44. Manser E, et al. PAK kinases are directly coupled to the PIX family of nucleotide exchange factors. Mol Cell. 1998; 1:183–192. [PubMed: 9659915]
45. Manser E, Leung T, Salihuddin H, Zhao ZS, Lim L. A brain serine/threonine protein kinase activated by Cdc42 and Rac1. Nature. 1994; 367:40–46. [PubMed: 8107774]
46. Takesono A, Horai R, Mandai M, Dombroski D, Schwartzberg PL. Requirement for Tec kinases in chemokine-induced migration and activation of Cdc42 and Rac. Curr Biol. 2004; 14:917–922. [PubMed: 15186750]

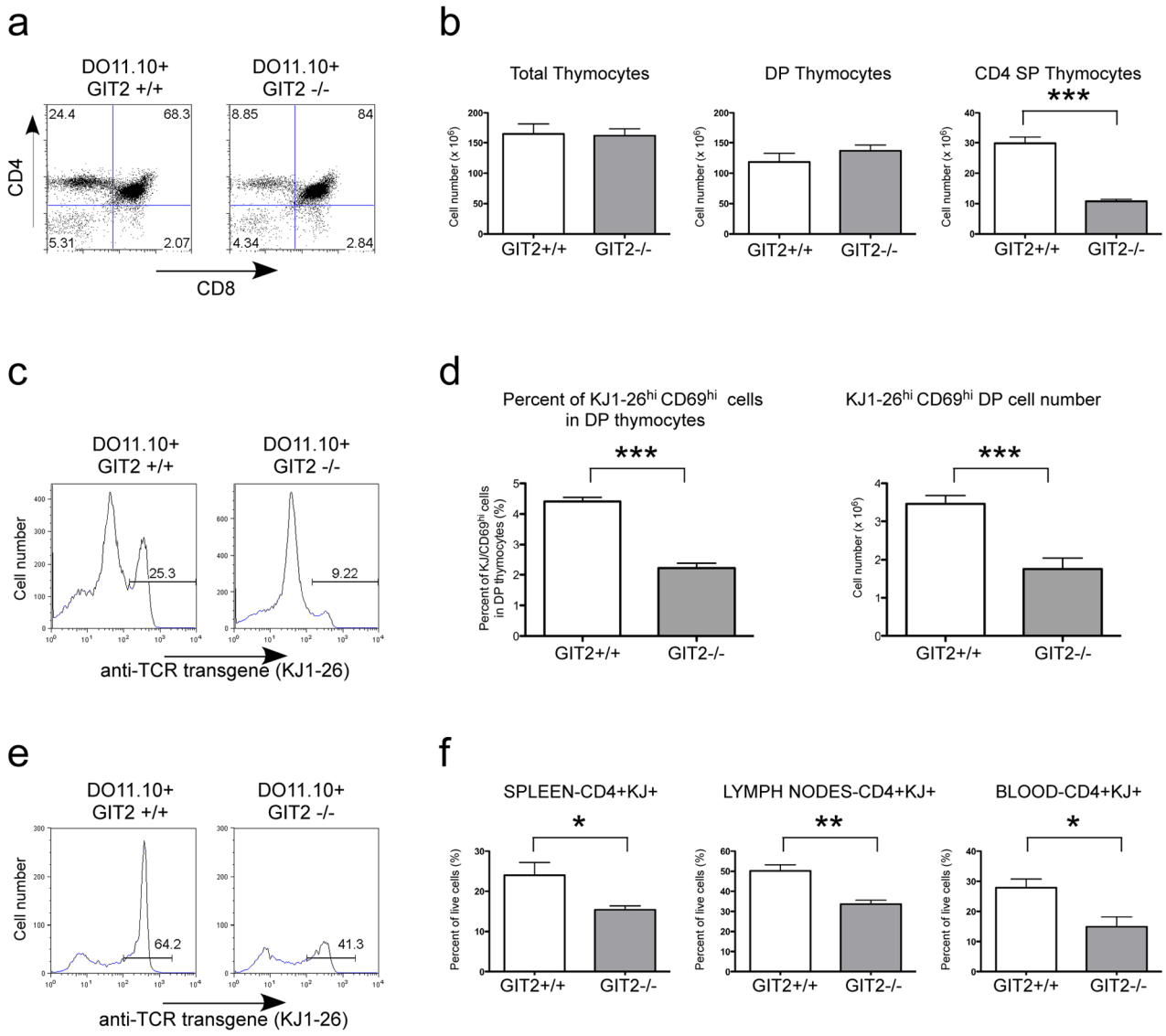

Figure 1. Impaired generation of CD4 SP thymocytes in DO11.10+ GIT2$^{-/-}$ mice

(**a**) Representative FACS analysis of CD4 and CD8 expression on thymocytes from DO11.10+ WT and DO11.10+ GIT2$^{-/-}$ mice to assess stages of thymocyte development. Numbers in each quadrant represent the percentage of cells in the indicated quadrant. (**b**) Quantification of cell numbers of different thymic subsets from DO11.10+ WT or DO11.10+ GIT2$^{-/-}$ mice. Error bars: s.e.m. (n=10–11 mice per genotype). (**c**) Expression of TCR transgene assessed by transgene specific antibody (KJ1-26) in total thymocytes from DO11.10+ WT or DO11.10+ GIT2$^{-/-}$ mice. (**d**) Percent of KJ1-26^{hi} CD69^{hi} cells in DP thymocytes and KJ1-26^{hi} CD69^{hi} DP cell number from DO11.10+ WT or DO11.10+GIT2$^{-/-}$ mice. Error bars: s.e.m. (n=3 mice per genotype). (**e**) Expression of KJ1-26 in CD4 T cells from DO11.10+ WT or DO11.10+ GIT2$^{-/-}$ spleen. (**f**) Percent of CD4^{+} KJ1-26^{+} cells in the periphery. (**e**,**f**) Graphs in this figure show mean ± s.e.m. (DO11.10+ WT mice, n=3; DO11.10+ GIT2$^{-/-}$ mice, n=5) *, $0.01 < P < 0.05$; **, $0.001 < P < 0.01$; ***, $P < 0.001$ (unpaired two-tailed Student's *t*-test).

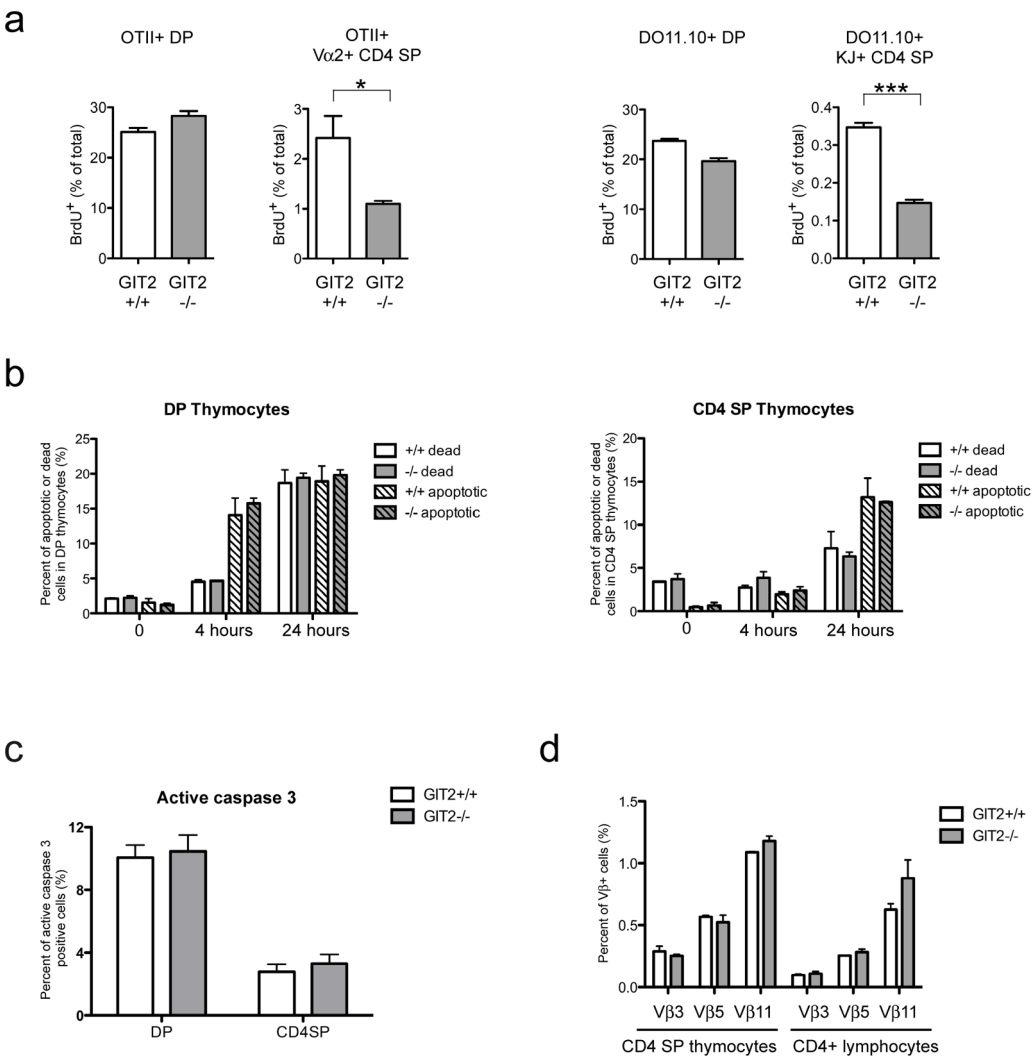

Figure 2. Reduced cell number in CD4 SP thymocytes from TCR transgenic GIT2$^{-/-}$ mice is due to impaired positive selection, not due to increased apoptosis or negative selection

(**a**) Intracellular staining of BrdU^{+} cells after 48 hours of BrdU incorporation using TCR transgenic WT or GIT2$^{-/-}$ mice. Thymocytes were labeled continuously with BrdU, as described in the Methods section. BrdU incorporation within the DP or CD4 SP thymocytes is plotted as a percentage of total live thymocytes (error bars: s.e.m.). Eight mice for OTII+ WT, six mice for OTII+ GIT2$^{-/-}$, three mice for DO11.10+ WT or DO11.10+ GIT2$^{-/-}$ were used. (**b**) Apoptosis assay using 7AAD/Annexin V staining at 0, 4, 24 hours of incubation in 10% FBS containing media in DO11.10+WT or DO11.10+ GIT2$^{-/-}$ thymocytes. Data are representative of two independent experiments using two or three mice per genotype for each experiment. (**c**) Intracellular staining of active caspase 3 in DO11.10+WT or GIT2$^{-/-}$ thymocytes. Data are pooled from two independent experiments using five mice for each genotype. (**d**) Percentages of Vβ3, Vβ5 and Vβ11 positive cells in CD4 SP thymocytes or CD4+ T cells from lymph nodes from BALB/c background WT and GIT2$^{-/-}$ mice are shown (error bars: s.e.m.; n=3 per each genotype). *, $0.01 < P < 0.05$; **, $0.001 < P < 0.01$; ***, $P < 0.001$ (unpaired two-tailed Student's *t*-test).

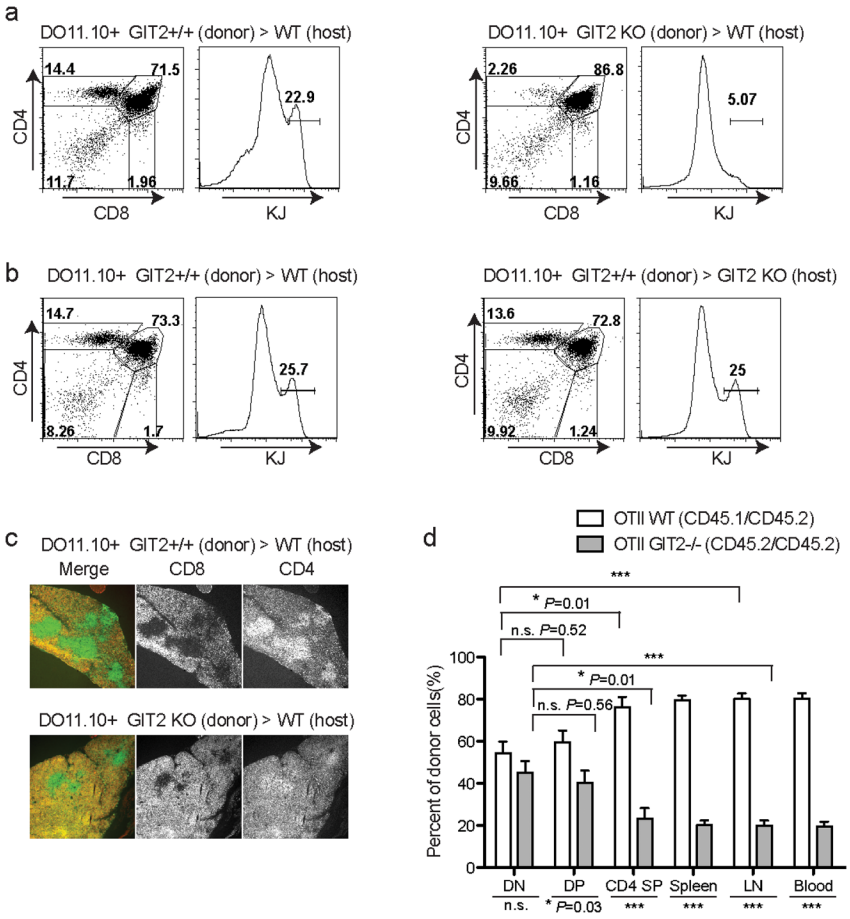

Figure 3. Defect in positive selection of TCR transgenic GIT2$^{-/-}$ thymocytes is hematopoietic cell intrinsic

(**a**) FACS analysis of WT BALB/c hosts reconstituted with DO11.10+WT or DO11.10+GIT2$^{-/-}$ donor bone marrow showing the defect in CD4 SP generation from DO11.10+GIT2$^{-/-}$ is hematopoietic cell intrinsic. Results are representative of three independent experiments. **(b)** FACS analysis of chimeras, in which WT and GIT2$^{-/-}$ hosts were reconstituted with DO11.10+WT bone marrow. Results are representative of five chimeras for each condition. (**c**) Thymic architecture of chimeras that were reconstituted with DO11.10+WT or DO11.10+GIT2$^{-/-}$ bone marrow cells. (**d**) One to one mixed bone marrow chimera using two different donor groups with different congenic markers (OTII +WT (CD45.1/CD45.2) and OTII+GIT2$^{-/-}$ (CD45.2/CD45.2)) revealed the defect in DP to CD4 SP transition in thymocytes generated from OTII+GIT2$^{-/-}$ bone marrow hematopoietic stem cells (HSCs). Results are pooled from seven independent experiments. Graphs in this figure show mean ± s.e.m. *, 0.01 < P < 0.05; **, 0.001 < P < 0.01; ***, P < 0.001 (unpaired two-tailed Student's t-test).

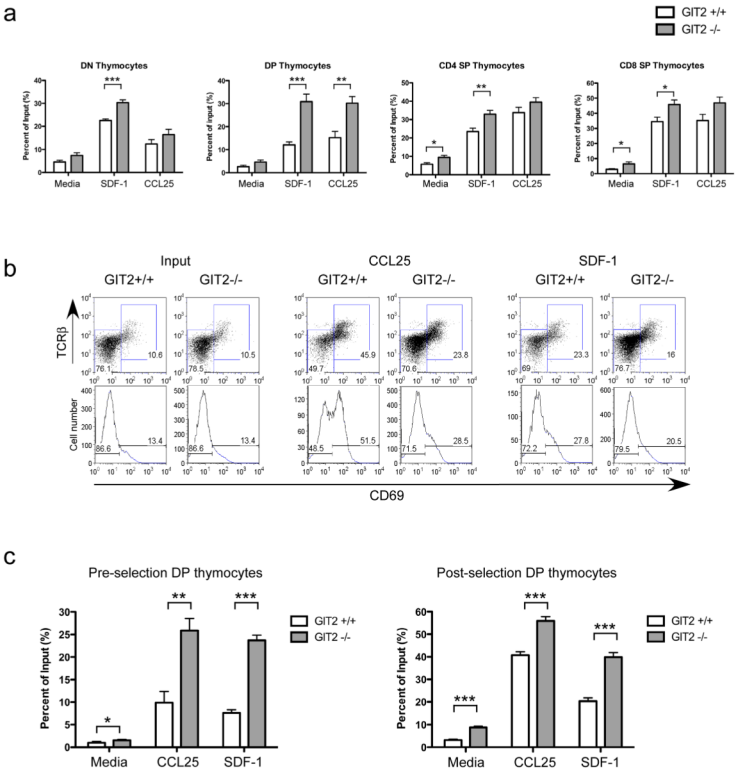

Figure 4. Increased migratory activity of GIT2$^{-/-}$ DP thymocytes in response to SDF-1 or CCL25

(**a**) Transwell migration assays were performed in the absence or presence of SDF-1 or CCL25 using WT and GIT2$^{-/-}$ thymocytes. Migrated thymocytes were collected, stained with anti-CD4 and CD8, and quantified using flow cytometry. Migration activity of distinct populations is presented as the percentage of input cells that migrated to the lower chamber. Bars indicate means and the standard errors of the means (s.e.m.) are indicated. Data are from five independent experiments with duplicates per condition. (**b**) Representative FACS analysis of CD69 and TCRβ expression (*upper panels*) or CD69 expression (*lower panels*) in DP populations of input or migrated thymocytes from WT or GIT2$^{-/-}$ mice in the presence of CCL25 or SDF-1. Migrated thymocytes were collected, stained with anti-CD4, CD8, CD69 and TCRβ, and quantified using flow cytometry. (**c**) Migration of pre-selection CD69^{low}TCRβ^{low} (*left*) and post-selection CD69^{hi}TCRβ^{hi} DP thymocytes (*right*) are presented as a percent of input. Data are from three independent experiments with duplicates per condition (error bars: s.e.m.). *, $0.01 < P < 0.05$; **, $0.001 < P < 0.01$; ***, $P < 0.001$ (unpaired two-tailed Student's *t*-test).

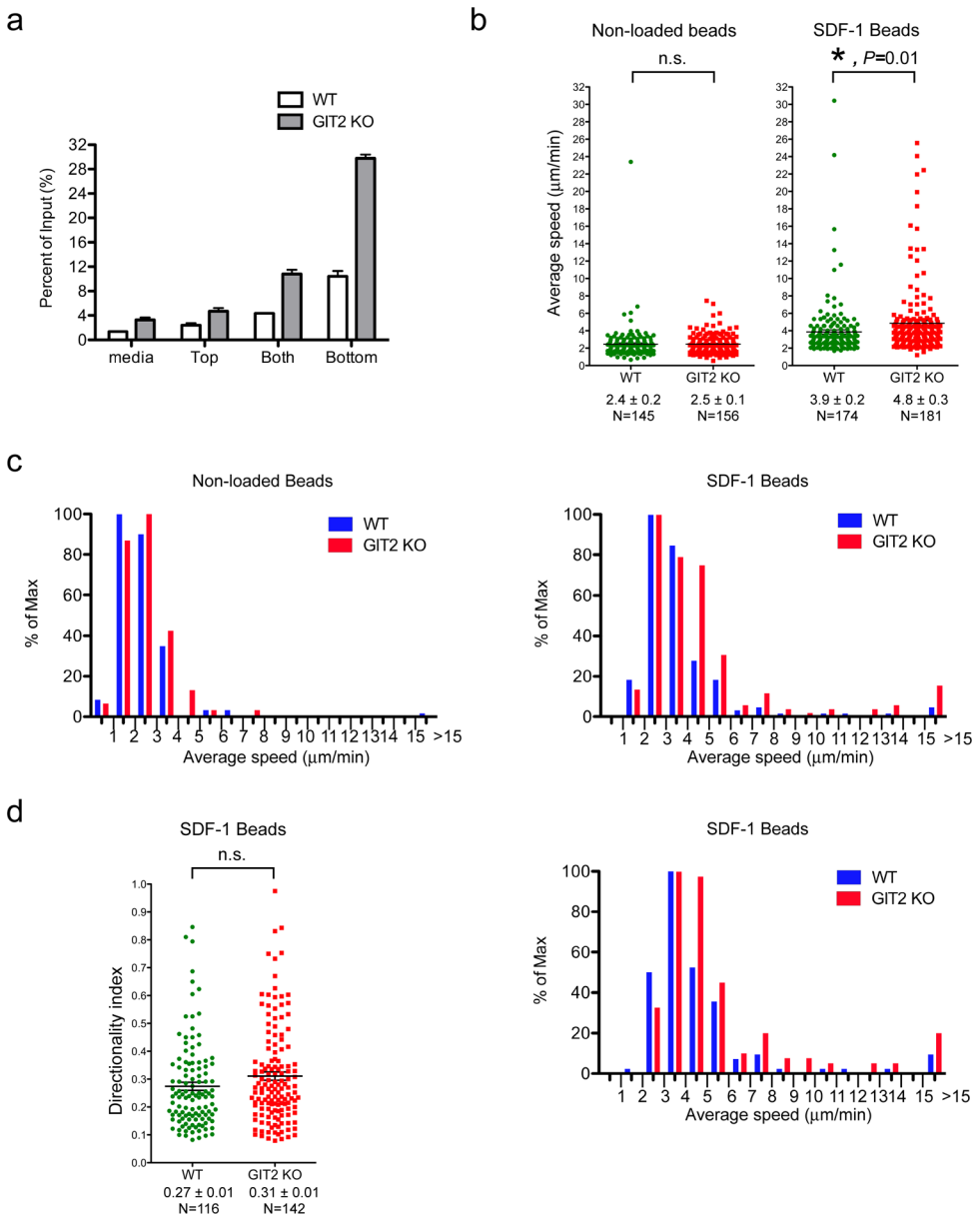

Figure 5. Increased directional and random motility of GIT2$^{-/-}$ thymocytes

(a) Transwell migration assays were performed with thymocytes in the upper well in the absence of SDF-1 (media) and in the presence of SDF-1 in the top well (Top), in the bottom well (Bottom), and in both top and bottom wells (Both) using WT and GIT2$^{-/-}$ thymcoytes. Results are representative of two independent experiments. (**b**) Directional migration of WT and GIT2$^{-/-}$ thymocytes on two-dimensional surfaces was monitored using SDF-1 releasing alginate beads and time-lapse fluorescence microscopy. WT and GIT2$^{-/-}$ thymocytes were labeled with CFSE (0.2 μM) and CMTMR (2 μM) respectively. A 1:1 mixture of thymocytes mixed plus 1.5 mg/ml collagen were placed on ICAM-1 (1 μg/ml) coated chambered coverglass in the presence of non-loaded (control) or SDF-1- loaded beads. Motility of WT (CFSE) and GIT2$^{-/-}$ (CMTMR) thymocytes were imaged for 40 min to 1 hour at 30 second intervals. Cell movement was measured based on the center of mass of GFP or CMTMR fluorescence using Imaris tracking software (Bitplane). To compare the

average migration speed (path length/time) of WT and GIT2$^{-/-}$ thymocytes in the presence of control beads or SDF-1-loaded beads, the average migration speed was calculated from cells based on two criteria. The first criterion required a displacement of more than 20 μm (about twice of cell length). The second criterion required the cell to be in the field for more than 500 sec if it did not move more than 20 μm. By using both criteria, almost all cells in the field in both conditions (beads only or SDF-1-loaded beads) were included for the analysis. Each dot represents a track of a thymocyte. Data are representative of two (control beads) and three (SDF-1 releasing beads) independent experiments. Graphs in this figure show mean ± s.e.m. (n.s.: not significant; *: P=0.03 (unpaired two-tailed Student's t-test)). (**c**) The average migration speed of WT and GIT2$^{-/-}$ thymocytes in the presence of control beads or SDF-1-loaded beads shown in (**b**) is binned into 1 μm/min intervals. Percentages of total cells that migrate within the particular range were measured and then normalized as a percentage of maximum (% of Max). (**d**) *Left panel*: The directionality index of WT and GIT2$^{-/-}$ thymocytes that migrate more than 20 μm towards SDF-1 releasing beads. Directionality index was determined by dividing displacement from origin by path length (n.s.: not significant, unpaired two-tailed Student's t-test). *Right panel*: To determine directional motility, the average migration speeds of WT and GIT2$^{-/-}$ thymocytes that moved towards SDF-1 releasing beads by more than 20 μm were binned into 1 μm/min intervals. For this analysis, cells that did not move towards SDF-1 releasing beads by more than 20 μm are excluded. Percentages of total cells that migrate within the particular range was measured and then normalized as a percentage of maximum (% of Max). Data are representative of three independent experiments.

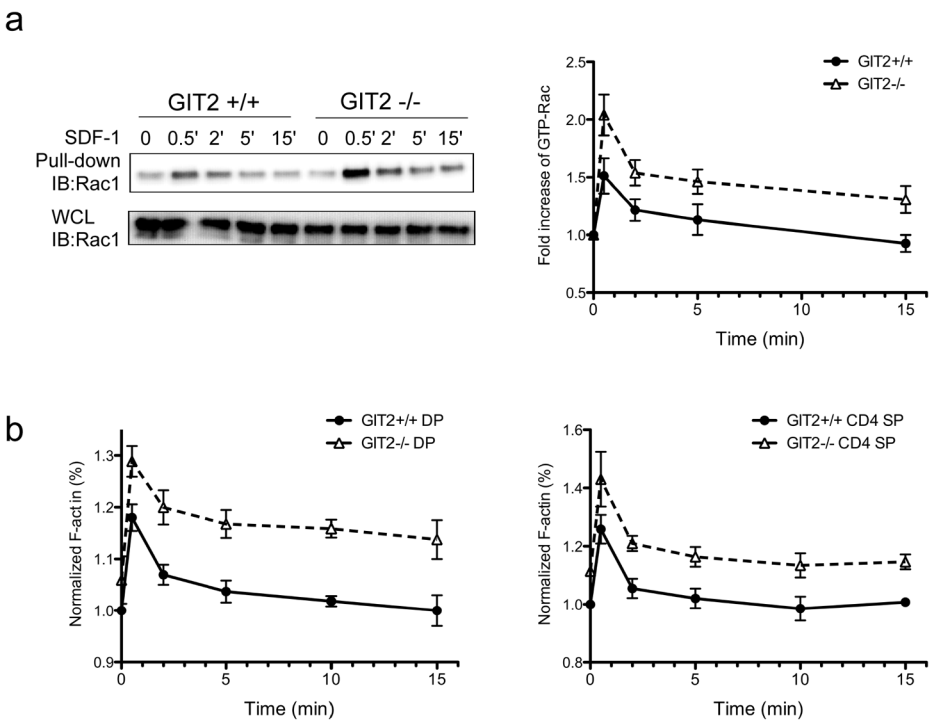

Figure 6. Increased Rac1 activation and actin polymerization in response to SDF-1 in GIT2$^{-/-}$ thymocytes

(**a**) Increased activation of Rac1 after 0, 0.5, 2, 5, 15 min of SDF-1 stimulation using WT or GIT2$^{-/-}$ thymocytes (*left*) WCL; whole cell lysates; Fold increase in Rac1 activation normalized to GTP-Rac1 in the resting state (*right*). (**b**) Increased actin polymerization in response to SDF-1 in GIT2$^{-/-}$ thymocytes as assessed by phalloidin-Alexa488, CD4 and CD8 staining. The mean fluorescence intensity of phalloidin-Alexa488 was measured in the DP (*left*) and CD4 SP (*right*) thymocyte populations and normalized to the value of WT at rest. Data are from three independent experiments per condition (error bars: s.e.m.).

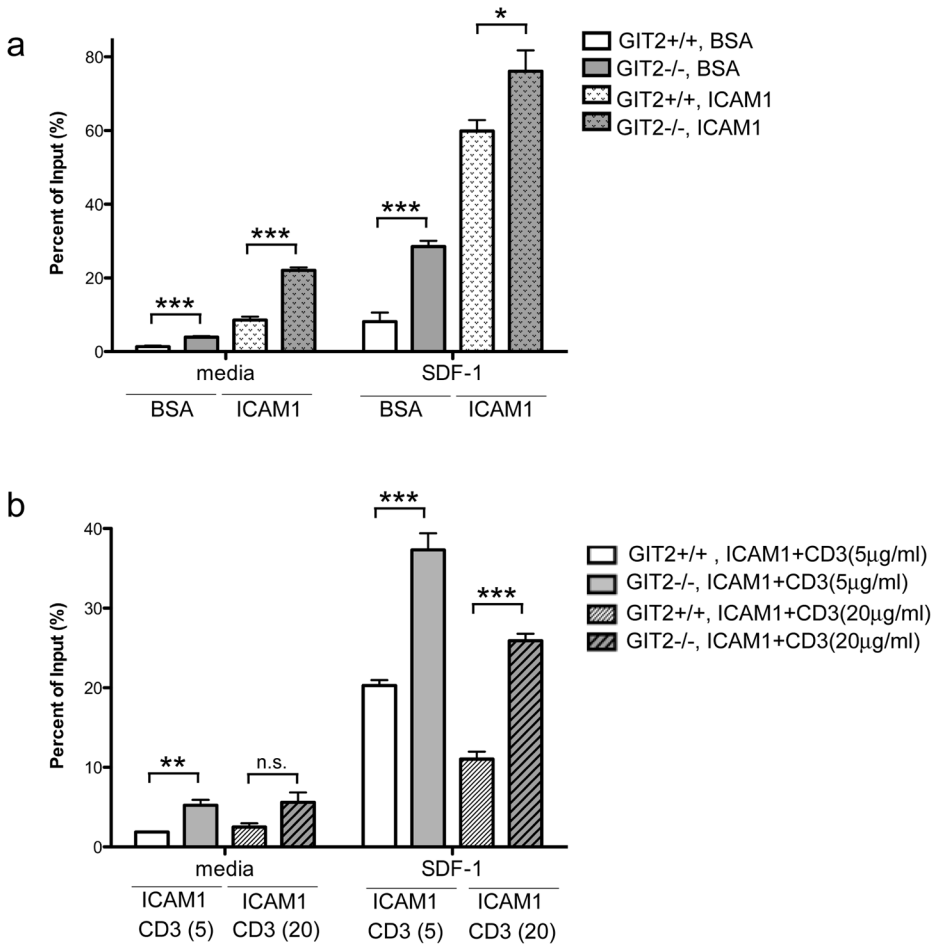

Figure 7. More GIT2$^{-/-}$ DP thymocytes overcome TCR-mediated stop signal in the presence of SDF-1

(**a**) Filters of transwells were coated with either 100μl of PBS alone or PBS containing ICAM-1 (3 μg/ml). Migration activity of WT or GIT2$^{-/-}$ thymocytes in the absence or presence of SDF-1 was measured using BSA- or ICAM-1- coated filters. Migrated thymocytes were collected, stained with anti-CD4 and CD8, and quantified using flow cytometry. Migratory activity of DP population is presented as a percentage of migrating DP cell number divided by input DP cell number. (**b**) Filters of transwells were coated with 100 μl of PBS containing ICAM-1 (3 μg/ml) plus two concentrations of CD3 (5 μg/ml or 20 μg/ml). Migratory activity of WT or GIT2$^{-/-}$ thymocytes in the absence or presence of SDF-1 was measured. Data are from two independent experiments with duplicates per condition (error bars: s.e.m.). *, $0.01 < P < 0.05$; **, $0.001 < P < 0.01$; ***, $P < 0.001$ (unpaired two-tailed Student's *t*-test).

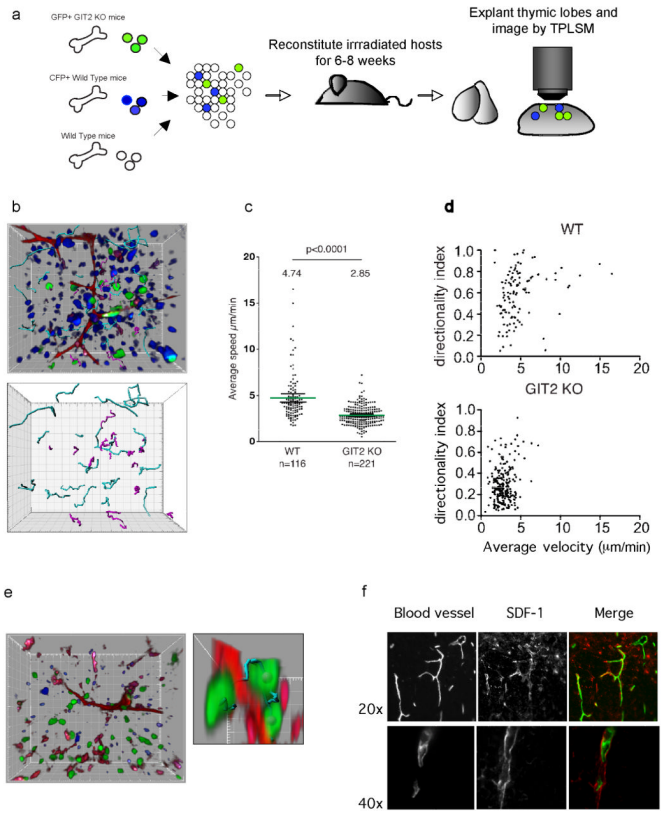

Figure 8. Altered motility of GIT2$^{-/-}$ thymocytes in the cortex

(**a**) Schematic diagram of the experimental set-up. Bone marrow cells from GIT2$^{-/-}$ mice expressing a GFP transgene under the control of the ubiquitin promoter (UBI-GFP) and WT mice expressing a CFP transgene under the control of actin promoter (Actin-CFP) were mixed with WT bone marrow cells, then transferred to irradiated hosts to generate partial hematopoietic chimeras in which about 1% of thymocytes are derived from the GFP-or CFP- expressing donor. After 6–8 weeks, intact thymic lobes from adult chimeric mice were imaged using TPLSM. (**b**) *Upper panel:* CFP (WT, blue) and GFP (GIT2$^{-/-}$, green) thymocyte images from thymi of a partial mixed bone marrow chimera at a single time point superimposed on cell tracks. Red: blood vessels. *Lower panel*: Trajectories of individual cells are shown as tracks. Yellow (CFP+ WT thymocytes), Purple (GFP+ GIT2$^{-/-}$ thymocytes). (**c**) Average migration speed (path length/time) of WT and GIT2$^{-/-}$ thymocytes. Each dot represents an individual tracked thymocytes. Data are compiled from one run for WT and three runs on two different days of imaging for GIT2$^{-/-}$. ***: P<0.0001 (unpaired two-tailed Student's t-test). (**d**) Directionality index (displacement/path length) plotted as a function of average speed (0–10 μm/min) of WT and GIT2$^{-/-}$ thymocytes. Average speeds of cells were binned between 2–3, 3–4 and 4–5 μm/min (grey line) and average directionality index of each bin is indicated (***, P=0.0004 for 2–3 μm/min speed; ***, P<0.0001 for 3–4 μm/min speed; ***, P<0.0001 for 4–5 μm/min speed, unpaired two-tailed Student's t-test). (**e**) Example of GIT2$^{-/-}$ thymocytes migrating near blood vessels. Fluorescent image is a projection of single time point with cell tracks superimposed. (**f**) Immunofluorescence of anti-SDF-1 staining in the thymus, showing SDF-1 positive blood vessels. Thymic sections injected with lectin-FITC to label blood vessels were stained for SDF-1 (*Upper panel:* 20x, *Lower panel:* 40x magnification).